Earth and Planetary Science Letters 272 (2008) 591–599

Contents lists available at ScienceDirect

Earth and Planetary Science Letters

journal homepage: www.elsevier.com/locate/epsl

Effects of physical erosion on chemical denudation rates: A numerical modeling study of soil-mantled hillslopes

Ken L. Ferrier [a,b,*], James W. Kirchner [a,c,d]

[a] Department of Earth and Planetary Science, University of California, Berkeley, United States
[b] Center for Accelerator Mass Spectrometry, Lawrence Livermore National Laboratory, Livermore, CA, United States
[c] Swiss Federal Institute for Forest, Snow, and Landscape Research (WSL), Birmensdorf, Switzerland
[d] Department of Environmental Sciences, Swiss Federal Institute of Technology, (ETH), Zürich, Switzerland

ARTICLE INFO

Article history:
Received 29 November 2007
Received in revised form 19 May 2008
Accepted 21 May 2008
Available online 4 June 2008

Editor: R.W. Carlson

Keywords:
chemical weathering
physical erosion
denudation
cosmogenic nuclides

ABSTRACT

Many biogeochemical and Earth surface processes depend critically on chemical weathering. The immediate products of chemical weathering are present as solutes and secondary minerals in groundwater, soils, and streams, and form the nutritional foundation for terrestrial biogeochemistry. Chemical weathering also contributes to physical erosion by weakening bedrock and producing easily erodible regolith, and as the primary long-term sink for atmospheric CO_2 it modulates Earth's long-term climate via the greenhouse effect. Long-term chemical denudation rates on soil-mantled hillslopes can be estimated from cosmogenic radionuclide (CRN) concentrations in soil-borne quartz and the enrichment of a chemically inert tracer in soil relative to its parent bedrock, a technique that inherently assumes steady physical erosion over the timescale of CRN accumulation. We present a numerical model that computes changes in soil mineralogy and CRN concentrations under time-varying physical erosion rates, and we use this model to assess the accuracy of the CRN-based technique for estimating chemical denudation rates in non-steady conditions.

Our modeling results suggest that CRN-based estimates of chemical denudation rates closely resemble actual chemical denudation rates averaged over the timescale of CRN accumulation, even during large-amplitude and long-period oscillations in physical erosion rates. For example, this model predicts that when physical erosion rates fluctuate sinusoidally by 50% of their mean over any period in time, CRN-based estimates of chemical denudation rates should differ from actual chemical denudation rates by less than 15%. Our model also implies that chemical denudation rates should approach zero both when physical erosion rates approach zero (because soluble minerals become depleted in the soil) and when physical erosion rates approach the maximum soil production rate (because soil thickness approaches zero). Modeled chemical denudation rates thus reach a maximum at intermediate physical erosion rates. If this relationship holds in nature, it implies that in rapidly eroding regions, further increases in physical erosion rates (e.g., due to increases in tectonic uplift rates) may not necessarily lead to faster chemical denudation on soil-mantled hillslopes.

Published by Elsevier B.V.

1. Introduction

Consider a scientist standing on a ridge overlooking a catchment. Under her feet the soil hosts a diverse biotic community, and the landscape below her is furrowed by ridges and valleys with streams flowing down the valley axes. All of these features of the catchment, both living and inanimate, depend on chemical weathering. Dissolved mineral constituents (the immediate products of chemical weathering) are present as cations and anions in ground and surface waters, and provide mineral-derived nutrients for organisms living in the soil and streams. Chemical weathering thus contributes to the nutritional foundation for terrestrial biogeochemistry. The geomorphic processes that sculpt the landscape also depend on chemical weathering, which converts bedrock to erodible regolith and thus accelerates landscape evolution. Chemical weathering of silicate minerals is the dominant sink for atmospheric CO_2 over geologic time (Walker et al., 1981; Berner et al., 1983), so to the degree that silicate weathering rates increase with temperature, they create a feedback loop that regulates Earth's long-term surface temperature via the greenhouse effect. Chemical weathering thus plays a critical role in many Earth surface processes across a wide range of timescales. In order to understand how these processes respond to various environmental factors (e.g., temperature, precipitation, pH), it is necessary to measure how these factors influence chemical weathering rates. This in turn requires the ability to measure chemical weathering rates accurately.

Several different approaches have been used to measure chemical weathering rates. Mineral dissolution rates have often been measured in laboratory experiments (e.g., Busenberg and Clemency, 1976; Chou and Wollast, 1984; White et al., 1999a; White and Brantley, 2003), an

* Corresponding author.
E-mail address: ferrier@eps.berkeley.edu (K.L. Ferrier).

0012-821X/$ – see front matter. Published by Elsevier B.V.
doi:10.1016/j.epsl.2008.05.024

approach that allows tight control over the weathering environment, and thus has the ability to isolate specific weathering mechanisms. Laboratory weathering experiments, however, are conducted over timescales much shorter than the natural timescales of mineral weathering, and the rates derived from these short-term studies are often several orders of magnitude faster than those derived from longer-term field studies (e.g., White and Brantley, 2003). This suggests that laboratory-derived rates cannot be applied directly to natural weathering environments, and highlights the need for field-based measurements of chemical weathering rates. At the catchment scale, field-derived chemical weathering rates were first determined by Garrels and Mackenzie (1967), based on the assumption that chemical weathering accounts for the difference in solute fluxes into and out of a catchment. Two decades later, Brimhall and Dietrich (1987) showed that measurements of mobile and immobile element concentrations in regolith and parent bedrock could be combined to yield chemical weathering rates averaged over the age of the soil. This technique requires sampling datable soils that have undergone negligible physical erosion (e.g., marine terraces (Brimhall et al., 1992) or river terraces (White et al., 1996), and thus is difficult to apply to actively eroding landscapes that lack such soils. In 1997, Kirchner et al. (1997) proposed that chemical denudation rates can be determined in actively eroding landscapes using measurements of denudation rates inferred from concentrations of in-situ produced cosmogenic radionuclides (CRN) in quartz, combined with measurements of immobile element enrichment in regolith relative to its parent bedrock. Subsequent studies (Riebe et al., 2001b, 2003, 2004a, b) demonstrated the accuracy of this technique and applied it to landscapes spanning a wide range of climates. This technique has two major strengths: (1) it can be applied to a wide range of landscapes because it does not require a datable non-eroding soil, and (2) it gives insight into soil formation and landscape evolution processes, because it is intrinsically averaged over the long timescales of soil formation and denudation. This method assumes that:(1) the soil mineralogy is derived solely from the bedrock beneath it (i.e., that any contamination of the soil by minerals from external sources such as windblown volcanic ash is negligible); (2) the soil has been representatively sampled; (3) the rock and soil contain an immobile tracer (element or mineral) that is so resistant to chemical dissolution that it is effectively lost from the soil only through physical erosion; and (4) the soil maintains a steady-state mass per unit area over the timescale of CRN accumulation (typically >1000 yr on eroding hillslopes).

In this paper, we examine the degree to which deviations from this steady-state assumption affect chemical denudation rates inferred from the technique of Kirchner et al. (1997) and Riebe et al. (2001b, 2003, 2004a,b). We approach this problem by modeling how mineral abundances and cosmogenic radionuclide concentrations in the soil evolve through time, imposing time-varying physical erosion rates on the model, and calculating the resulting variations in inferred chemical denudation rates.

2. Theory

2.1. Chemical denudation rates inferred from concentrations of cosmogenic radionuclides and immobile elements

Consider a hillslope soil which undergoes steady-state formation and denudation such that it maintains a constant mass per unit area over time (Fig. 1). On such a steady-state hillslope, the soil production rate ϵ_b equals the denudation rate D, which itself equals the sum of the physical erosion rate E and chemical denudation rate W:

$$\epsilon_b = D = E + W. \tag{1}$$

Here ϵ_b, D, E, and W all have dimensions of mass per unit area of hillslope per time. We describe W as a chemical denudation rate and not a chemical weathering rate to emphasize that W connotes transport of dissolved mineral constituents out of the soil, and not merely chemical alteration of minerals. If secondary minerals precipitate in the soil, then the chemical denudation rate W is the difference between the sum of all primary mineral dissolution rates and all secondary mineral precipitation rates. Conservation of mass for an individual mineral or element X dictates that

$$D \cdot [X]_r = E \cdot [X]_s + W_X, \tag{2}$$

where $[X]_r$ and $[X]_s$ are the average concentrations [mol M^{-1}] of X in rock and soil, respectively, and W_X is the chemical denudation rate of X [mol L^{-2} T^{-1}] per unit area of hillslope, not unit mineral surface area. In using this equation, we assume that changes in the soil composition by aeolian deposition and convergence or divergence of soil from upslope (e.g., Mudd and Furbish, 2006) are negligible. If X is an element or mineral that is so resistant to dissolution that its chemical denudation rate W_X is negligible, it is termed "immobile" and Eq. (2) yields an expression for E in terms of the denudation rate and the average immobile element concentrations in the rock and soil.

$$E = D\frac{[Zr]_r}{[Zr]_s} \tag{3}$$

Here we have chosen zirconium as an example of a commonly-used immobile element. This expression can be substituted into Eq. (1) to yield the following expression for chemical denudation rate W.

$$W = D\left(1 - \frac{[Zr]_r}{[Zr]_s}\right) \tag{4}$$

Eq. (3) can similarly be substituted into Eq. (2) to yield an expression for the chemical denudation rate of an individual element or mineral X.

$$W_X = D\left([X]_r - [X]_s\frac{[Zr]_r}{[Zr]_s}\right) \tag{5}$$

At this point it is necessary to distinguish between instantaneous rates and inferred rates. We define the instantaneous denudation rate

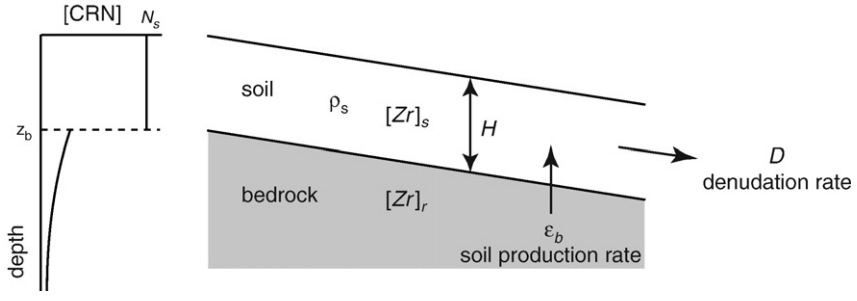

Fig. 1. In the idealized soil-mantled hillslope pictured here, soil is produced at the soil–bedrock boundary at a rate ϵ_b and is lost downslope at a denudation rate D. In steady state, soil production rates match denudation rates, and the mass of soil per unit area (given by soil density ρ_s times soil thickness H) is constant in time. For a steady-state hillslope such as this, it is possible to infer chemical denudation rates by combining measurements of cosmogenic radionuclide (CRN) concentrations in the soil with measurements of the average immobile element concentrations in soil and its parent bedrock ($[Zr]_s$ and $[Zr]_r$, respectively).

D_{inst} as the denudation rate at any moment in time. It is distinct from the inferred denudation rate D_{inf}, which in practice may be calculated from measurements of cosmogenic radionuclide concentrations in soil-borne quartz, as described below. Similarly, the instantaneous chemical denudation rate W_{inst} is the chemical denudation rate at any moment in time, while the inferred chemical denudation rate W_{inf} is that calculated with Eq. (4), as described above. To emphasize that the chemical denudation rate in Eq. (4) is an inferred rate, we rewrite Eq. (4) with the inferred variables D_{inf} and W_{inf}.

$$W_{inf} = D_{inf}\left(1-\frac{[Zr]_r}{[Zr]_s}\right) \tag{6}$$

In practice, CRN concentrations may be used to infer the denudation rate D_{inf}, as in Eq. (7) (Lal, 1991):

$$D_{inf} = \frac{P_0 \Lambda}{N_s}. \tag{7}$$

Here D_{inf} is the inferred denudation rate [M L^{-2} T^{-1}], P_0 is the surface production rate of CRN in quartz [atoms M^{-1} T^{-1}], N_s is the measured concentration of CRN in quartz [atoms M^{-1}], and Λ [M L^{-2}] is the so-called penetration depth of cosmic-ray neutrons, an exponential scaling constant that describes how quickly the cosmic-ray neutron flux is attenuated as it passes through matter. Note that in Eqs. (2)–(7), $[Zr]_s$, $[X]_s$, and N_s are the average concentrations of Zr, X, and N_s in the soil, which means that from a practical standpoint the entire soil column must be sampled to obtain representative average concentrations. This equation assumes that muogenic production of CRN and radioactive decay of CRN are both negligible contributors to the overall CRN budget in the soil. For the shallow and continually-eroding soils we are modeling these are justifiable assumptions; in the upper meter below the Earth's surface, muogenic production of CRN accounts for less than 3% of the total (Stone et al, 1998), and the residence time of quartz grains within the penetration depth of CRN-producing nucleons is, for our model conditions, <2% of the 1.5 Myr half-life of the commonly-used CRN ^{10}Be. For CRN with much shorter half-lives, such as ^{14}C, losses to radioactive decay are significant and Eq. (7) is inaccurate; for this reason our analysis is restricted to CRN that have long half-lives or are stable (e.g., ^{10}Be, ^{26}Al, ^{3}He, ^{21}Ne). We note that muogenic production of CRN is significant in rapidly eroding sites at low elevations (see Balco et al., 2008 for discussion), and we ignore it because muogenic corrections to CRN-derived denudation rates are small for the high-elevation sites where this technique has most often been applied (e.g., Riebe et al., 2001b), and because there is only a minor benefit in adding muogenic production to a model that is intended for exploring general patterns in chemical denudation rates, rather than comparing modeled CRN concentrations to measured CRN concentrations. Eq. (7) also ignores the effects of selective enrichment of quartz in the soil, which increases the exposure time of quartz to cosmic radiation and so artificially lowers inferred denudation rates (Small et al., 1999; Riebe et al., 2001a). Except in cases of extreme chemical weathering, this effect is small; Riebe et al. (2001a) showed that this process biases denudation rates by an average of only 6% for granitic soils in the Sierra Nevada under conditions similar to those that we model in this paper.

Inherent in the approach of Eq. (7) for measuring denudation rates – and hence in the approach of Eq. (6) for measuring chemical denudation rates – is an assumption of steady state; that is, it is assumed that denudation rates are constant over the timescale of CRN accumulation in quartz. In this paper, we are primarily concerned with quantifying the accuracy of this approach if denudation rates vary through time, making the assumption of steady state invalid. With this goal in mind, we created a numerical model that tracks the variables in Eq. (6) under time-varying physical erosion rates.

2.2. A model of chemical denudation rates in soil

In order to model the effects of non-steady physical erosion on chemical denudation rates inferred from Eq. (6), it is necessary to calculate the effects of non-steady physical erosion on immobile element concentrations in the soil and on inferred denudation rates over time. This requires tracking the time-varying concentrations of all minerals in the soil and cosmogenic radionuclide (CRN) concentrations in soil-borne quartz. Here we give a brief outline of the equations used to track these variables over time and list the assumptions upon which these equations rest. Full derivations of these equations are presented in the Supplementary data.

The model rests on several fundamental assumptions. First, we assume that the soil production rate ϵ_b depends exponentially on soil thickness H as in the formulation of Heimsath et al. (1997, 1999, 2000, 2001, 2005).

$$\epsilon_b = \epsilon_0 e^{-\alpha H} \tag{8}$$

Here ϵ_0 represents the soil production rate at zero soil thickness, and α [L^{-1}] is a constant that describes the exponential dependence of soil production rate on soil thickness. Second, we follow the approach of Chamberlain et al. (2005) in assuming that the dissolution rate of mineral phase X is a linear function of its specific surface area A_X [L^2 mol^{-1}] and its concentration in the soil $[X]_s$ [mol M^{-1}].

$$\frac{d[X]_s}{dt}(\text{mineral dissolution}) = -k_X A_X [X]_s \tag{9}$$

Here k_X is the dissolution rate constant [mol L^{-2} T^{-1}] for mineral phase X. Third, we assume, as in Chamberlain et al. (2005), that any given secondary mineral phase X is produced at a constant rate s_X [mol $L^{-3}T^{-1}$] per unit volume of soil. Fourth, we assume that CRN production rates decrease exponentially below the Earth's surface (Lal, 1991).

$$P(z) = P_0 e^{-\rho z/\Lambda} \tag{10}$$

Here $P(z)$ is the CRN production rate at depth z, P_0 is the CRN production rate at the surface, ρ is the density of the material (e.g., soil, rock) through which the cosmic-ray flux passes, and Λ is the penetration depth of cosmogenic gamma ray neutrons, expressed as mass per unit area. We also assume that changes in CRN concentrations due to radioactive decay, muogenic production, and downslope divergences in soil fluxes are all negligible. Lastly, we assume that mass is conserved during soil production and denudation. Given these assumptions, we derive the following differential equations for soil thickness, CRN concentrations and mineral concentrations.

Soil thickness H varies at a rate proportional to the imbalance between rates of soil production and soil denudation:

$$\frac{dH}{dt} = \frac{1}{\rho_s}\left(\epsilon_0 e^{-\alpha H} - E_{inst} - W_{inst}\right). \tag{11}$$

Here ρ_s is the density of soil and E_{inst} and W_{inst} are the instantaneous rates of physical erosion and chemical denudation. We impose a time-varying E_{inst} on the model, and allow all other variables to respond to it. E_{inst} drives the model.

Soil CRN concentrations N_s vary according to

$$\frac{dN_s}{dt} = \frac{1}{\rho_s H}\left(\epsilon_0 e^{-\alpha H}\left(N_{z_b} - N_s\right) + \Lambda P_0\left(1-e^{-\rho_s H/\Lambda}\right)\right), \tag{12}$$

where N_{z_b} is the CRN concentration in bedrock at the soil–bedrock boundary. Because soil thickness varies during non-steady denudation, N_{z_b} also varies in time:

$$\frac{dN_{z_b}}{dt} = P_0 e^{-\rho_s H/\Lambda} - \epsilon_0 e^{-\alpha H}\frac{N_{z_b}}{\Lambda}. \tag{13}$$

Lastly, soil mineral concentrations $[X]_s$ are given by

$$\frac{d[X]_s}{dt} = \frac{\epsilon_0 e^{-\alpha H}}{\rho_s H}\left([X]_r - [X]_s\right) + \frac{s_X}{\rho_s} - k_X A_X [X]_s + [X]_s \sum_{j=1}^{n}\left(k_j A_j [X_j]_s w_j - \frac{s_j w_j}{\rho_s}\right), \quad (14)$$

where $[X]_r$ is the concentration of mineral phase X in bedrock [mol M^{-1}], n is the number of mineral phases in the soil, $[X_j]_s$ is the concentration of the jth soil mineral phase in the summation [mol M^{-1}], and k_j, A_j, s_j, and w_j are the dissolution rate constant, specific surface area, secondary mineral production rate, and molar mass, respectively, of mineral phase X_j.

These assumptions also allow us to calculate instantaneous chemical denudation rates over time. Expressed in dimensions of [M L^{-2} T^{-1}], instantaneous chemical denudation rates are the difference between the sum of all mineral dissolution rates and all secondary mineral production rates.

$$W_{inst} = \sum_{j=1}^{n}\left(k_j A_j [X_j]_s w_j \rho_s H - s_j w_j H\right) \quad (15)$$

We use a fourth-order Runge–Kutta routine (Press et al., 1992) to numerically integrate Eqs. (11)–(14) over time. This allows us to calculate variations in soil CRN and mineral concentrations, from which we calculate variations in chemical denudation rates inferred with Eq. (6). Together, these equations comprise a useful tool for examining the influence of variable physical erosion rates on soils; we can impose an arbitrary temporal pattern in physical erosion rates on the soil and observe the responses in soil thickness, mineral concentrations, CRN concentrations, and chemical denudation rates.

3. Model results

How do modeled soils respond to variable rates of physical erosion? Fig. 2 shows the results of a model run in which we drive the model with a sinusoidal physical erosion rate E_{inst} whose magnitude varies by a factor of 5 over a 10,000-year period, and in which the bedrock has a granitic mineralogy consisting of 40% plagioclase feldspar, 24.99% quartz, 20% potassium feldspar, 15% biotite, and 0.01% zircon. Table C.1 in the Supplementary data lists all other parameter values used for this model run. In the top panel of Fig. 2 is the instantaneous physical erosion rate E_{inst}, which we impose on the model and which drives the variations in all other variables. In the lower panels are soil thickness, soil mineral concentrations, and instantaneous and inferred chemical denudation rates. Note that the resultant soil characteristics are similar to those in mountainous granitic soils: soil thickness oscillates between 21 and 37 cm, chemical denudation rates average 27% of the denudation rate, and the average soil mineralogy (34% quartz, 18% plagioclase, 26% K-feldspar, 3% biotite, and 18% kaolinite) is, as expected, depleted in soluble minerals (plagioclase and biotite) and enriched in less soluble minerals (quartz and K-feldspar) and secondary clays (kaolinite).

We can draw several conclusions from Fig. 2. First, the fluctuations in soil thickness, soil mineral concentrations, and chemical denudation rates are less pronounced than the fluctuations in physical erosion rates. All of the response variables are damped. Second, inferred chemical denudation rates W_{inf} are less variable in time than instantaneous chemical denudation rates W_{inst} as the bottom panel in Fig. 2 shows. This is not surprising; W_{inf} is intrinsically a time-averaged quantity because it is inferred from quantities that are themselves time-averaged and buffered against rapid changes in physical erosion rates — namely, concentrations of CRN and an inert tracer in the soil. Thus W_{inf} ought to be less variable in time than W_{inf}, and the model verifies that it is. Third, W_{inf} lags behind physical erosion rates; because W_{inf} is inferred from quantities that are buffered against sudden changes in physical erosion rates, it responds slowly to changes in physical erosion rates.

4. Generalization of model

The lower panel in Fig. 2 shows chemical denudation rates responding to one particular set of conditions governing rates of physical erosion and mineral dissolution, and it provokes several questions about the general behavior of W_{inf}. How does the amplitude of W_{inf} depend on the amplitude and period of the physical erosion rate driver E_{inst}? How does the response of W_{inf} depend on the values of rate constants for mineral dissolution and clay production? In order to answer these questions, we simplify and generalize the model by non-dimensionalizing Eqs. (6)–(15), and in so doing we eliminate the model's dependence on particular values for soil production parameters ϵ_0 and α and CRN production parameters P_0 and Λ. We leave the full derivation of the non-dimensional equations to the Supplementary data, and here simply point out two important elements of the non-dimensionalization. First, physical erosion rates and chemical denudation rates are scaled by the soil production coefficient ϵ_0, such that, e.g., the non-dimensional physical erosion rate $\hat{E}_{inst}$ is zero at $E_{inst}=0$ and $\hat{E}_{inst}$ is 1 at $E_{inst}=\epsilon_0$. Throughout this paper non-dimensional variables are denoted with a carat. Second, we scale time by a soil production timescale $T_p=\Lambda\epsilon_0^{-1}$, such that non-dimensional time $\hat{t}$ is given by

$$\hat{t} = \frac{t}{T_p} = \frac{t\epsilon_0}{\Lambda}. \quad (16)$$

Note that for the range of published values for ϵ_0, one unit of non-dimensional time t translates to a range of 4267–25,157 yr in real time,

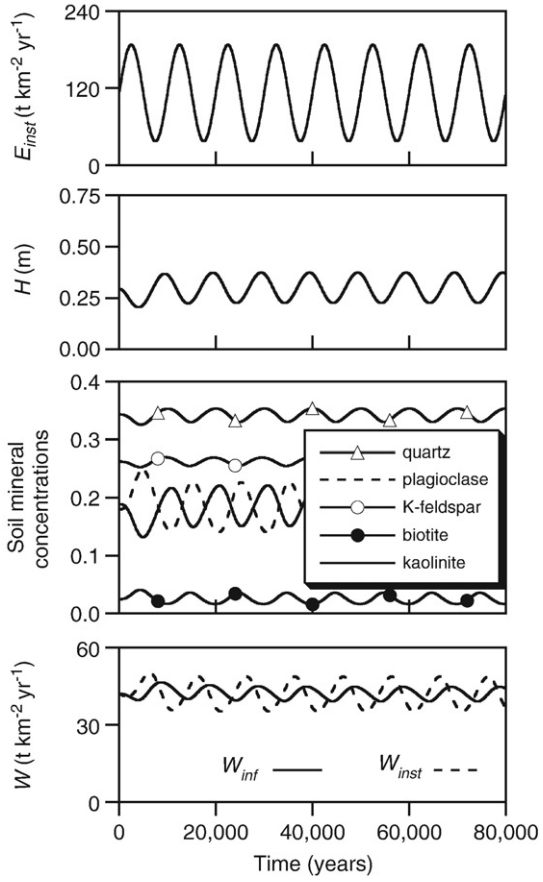

Fig. 2. Results of one model run. In the top panel is the instantaneous physical erosion rate E_{inst}, which we impose on the model and which drives variations in all other variables. In the lower panels are soil thickness H, soil mineral concentrations (in kg mineral/kg soil), and instantaneous and inferred chemical denudation rates W_{inst} and W_{inf}, calculated with Eqs. (15) and (6), respectively. In this model run we have set soil production constants to $\epsilon_0=375$ t km^{-2} yr^{-1} and $\alpha=3$ m^{-1} (Heimsath et al., 2001). Values for all other rate constants used in this model run are listed in Table C.1 in the Supplementary data.

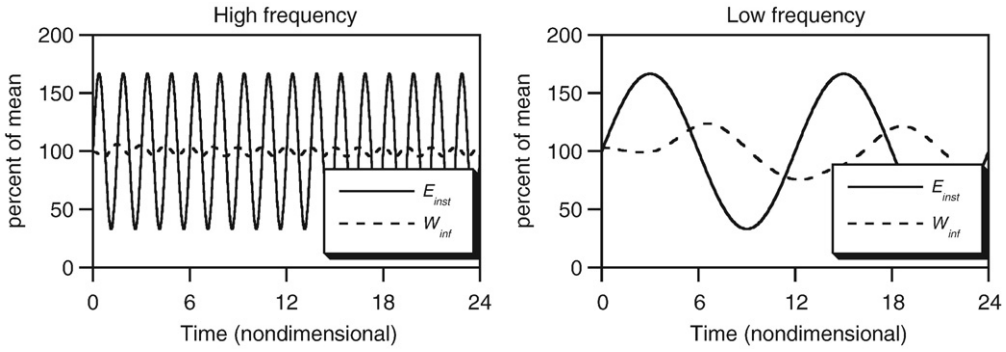

Fig. 3. Responses of inferred chemical denudation rates to two physical erosion rate patterns of the same amplitude and different periods. Each plot shows instantaneous physical erosion rates E_{inst} (imposed upon the model) and inferred chemical denudation rates W_{inf} (responding to E_{inst}) as percentages of their means over the course of a model run. Non-dimensional parameter values used in these runs are listed in Table C.2 in the Supplementary data. These figures suggest that inferred chemical denudation rates vary more widely under longer period oscillations in physical erosion rate.

for the Oregon Coast Range (Heimsath et al., 2001) and southeastern Australia (Heimsath et al., 2000), respectively.

5. Non-dimensional model results

5.1. How do the amplitude and period of fluctuations in physical erosion rates affect the stability of inferred chemical denudation rates?

The extent to which inferred chemical denudation rates deviate from their long-term mean should depend on the amplitude and period of the physical erosion rates that perturb them. In Fig. 3 we show two snapshots of the behavior of $\hat{W}_{inf}$ in response to two physical erosion rate patterns which share the same amplitude but have different frequencies. In each of these model runs, $\hat{W}_{inf}$ oscillates about its long-term mean with a characteristic amplitude. In the "high frequency" model run in Fig. 3, for example, where $\hat{E}_{inst}$ deviates from its mean by 67% and the non-dimensional period of $\hat{E}_{inst}$ is 1.5 (equivalent to 6400 yr given the value for ϵ_0 used in Fig. 2), the amplitude of $\hat{W}_{inf}$ is 6% of the mean $\hat{W}_{inf}$. This is the maximum deviation of $\hat{W}_{inf}$; at most moments during the model run, the deviation of $\hat{W}_{inf}$ is less than 6% of its mean. The model runs in Fig. 3 suggest that increasing the period of $\hat{E}_{inst}$ increases the amplitude of deviations in $\hat{W}_{inf}$.

We can create a more complete picture of the stability of inferred chemical denudation rates by plotting the amplitude of $\hat{W}_{inf}$ as a function of the amplitude and period in the physical erosion rate driver. The results are shown in Fig. 4. These show the amplitude of $\hat{W}_{inf}$, defined as the maximum deviation of W_{inf} from its mean over the course of the model run. Fig. 4(a)–(b) show that, as expected, chemical denudation rates fluctuate to a greater degree at large-amplitude oscillations in $\hat{E}_{inst}$ and at long-period oscillations in $\hat{E}_{inst}$. The fact that higher amplitude oscillations in $\hat{E}_{inst}$ cause higher amplitude oscillations in $\hat{W}_{inf}$ is not surprising; stronger forcing ought to induce a stronger response, and Fig. 4(a) shows that it does. Longer-period oscillations in physical erosion rates, on the other hand, produce larger oscillations in chemical denudation rates because $\hat{W}_{inf}$ takes time to respond to changes in $\hat{E}_{inst}$. During short-period oscillations in $\hat{E}_{inst}$, $\hat{W}_{inf}$ has little time to respond to changes in $\hat{E}_{inst}$, and so always remains close to its mean, whereas during long-period oscillations in $\hat{E}_{inst}$, $\hat{W}_{inf}$ has more time to adjust to swings in physical erosion rate, and thus deviates farther from its mean. All of this implies that $\hat{W}_{inf}$ is more stable at physical erosion rates that oscillate at shorter periods and smaller amplitudes.

5.2. How do inferred chemical erosion rates compare to actual chemical erosion rates?

The analysis in Section 5.1 shows how far inferred chemical denudation rates deviate from their long-term mean. When physical erosion rates oscillate with periods much longer than the timescale of CRN accumulation (e.g., in the "low frequency" example in Fig. 3), inferred chemical denudation rates stray far from their mean averaged over many oscillations, but do not stray as far from the mean chemical denudation rate averaged over the timescale of CRN accumulation — which is what we are trying to measure. How accurately do inferred chemical denudation rates mimic actual chemical denudation rates averaged over the CRN accumulation timescale?

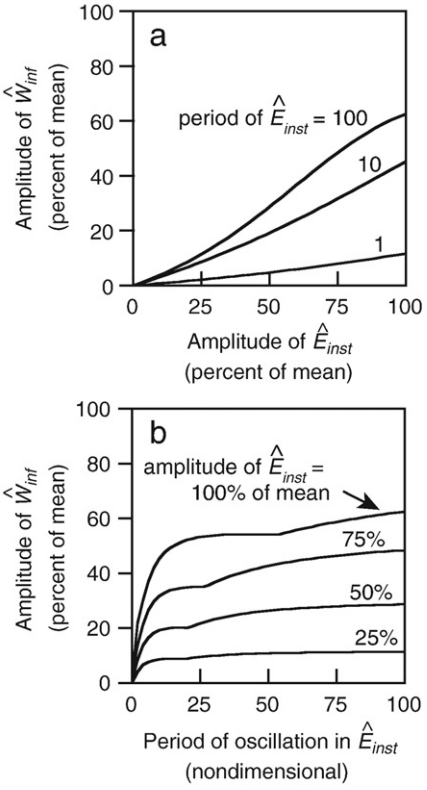

Fig. 4. (a) and (b) depict the amplitude of $\hat{W}_{inf}$ – defined as the maximum deviation of chemical denudation rates from their long-term mean – as a function of the amplitude and period of imposed oscillations in physical erosion rate $\hat{E}_{inst}$. (By way of example, in the "high frequency" panel of Fig. 3, in which $\hat{E}_{inst}$ has a non-dimensional period of 1.5 and an amplitude of 67% of the mean, the amplitude of $\hat{W}_{inf}$ is 6% of its mean.) Here, in Fig. 4, physical erosion rates oscillated around a mean $\hat{E}_{inst}$ of 0.35. Non-dimensional parameter values used in these runs are listed in Table C.2 in the Supplementary data. These figures indicate that inferred chemical denudation rates fluctuate to a greater degree under high-amplitude and long-period oscillations in physical erosion rate. Even under very high amplitude and very long-period oscillations in $\hat{E}_{inst}$, however, $\hat{W}_{inf}$ is less variable than $\hat{E}_{inst}$.

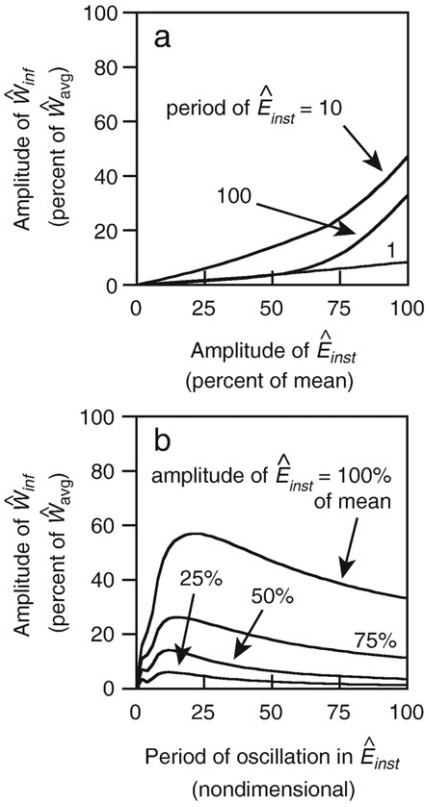

Fig. 5. These show the degree to which inferred chemical denudation rates $\hat{W}_{inf}$ deviate from $\hat{W}_{avg}$, where $\hat{W}_{avg}$ is the mean chemical denudation rate averaged over the CRN accumulation timescale. Non-dimensional parameter values used in these runs are listed in Table C.2 in the Supplementary data. Note that the amplitudes of $\hat{W}_{inf}$ in Fig. 5 are smaller than in Fig. 4; this indicates that deviations of $\hat{W}_{inf}$ from $\hat{W}_{avg}$ are smaller than deviations of $\hat{W}_{inf}$ from the mean chemical denudation rate averaged over many oscillations in physical erosion rates. $\hat{W}_{inf}$ is thus a more accurate estimate of chemical denudation rates averaged over the CRN accumulation timescale than over the period of oscillation in physical erosion rates.

We answer this question by defining a new variable, W_{avg}, as the mean chemical denudation rate averaged over the CRN accumulation timescale T_{CRN}. On a steadily eroding hillslope, T_{CRN} can be calculated as the penetration depth of cosmic-ray neutrons divided by the inferred denudation rate.

$$T_{CRN} = \frac{\Lambda}{D_{inf}} \tag{17}$$

This timescale depends on the value of D_{inf}, which itself changes as CRN concentrations fluctuate in response to fluctuations in physical erosion rates. In the model run in Fig. 2, for example, T_{CRN} oscillates between 9185 and 10,840 yr. At each moment during a model run, we calculate W_{avg} as the average of all instantaneous chemical denudation rates W_{inst} stretching back over the previous T_{CRN} years. In this manner we can compare inferred chemical denudation rates (W_{inf}) to actual chemical denudation rates averaged over the timescale of CRN accumulation (W_{avg}), as Fig. 5 shows. A comparison of Fig. 5 with Fig. 4 shows that inferred chemical denudation rates mimic W_{avg} more accurately than they mimic the mean chemical denudation rate averaged over many oscillations in physical erosion rate. During the largest possible swings in physical erosion rates – i.e., 100% of the mean – W_{inf} may deviate from W_{avg} by as much as 57% (Fig. 5), but this deviation drops off quickly at smaller amplitude oscillations in physical erosion rates. When physical erosion rates oscillate by 50% of their mean, for example, W_{inf} deviates from W_{avg} by no more than 15%. These errors are not negligible, but they are small for field-derived measurements of chemical denudation rates averaged over millennial timescales.

5.3. How do mineral dissolution rates and clay mineral production rates affect the stability of inferred chemical denudation rates?

The literature records a wide range of published rate constants for mineral dissolution and clay production (see, e.g., reviews by White and Brantley, 2003 and Price et al., 2005). How does the choice of rate constants affect the degree to which $\hat{W}_{inf}$ deviates from its mean? In Fig. 6 we show the maximum amplitude of $\hat{W}_{inf}$ – defined as in Section 5.2 as the maximum deviation of $\hat{W}_{inf}$ from $\hat{W}_{avg}$ – as a function of the non-dimensional rate constants for mineral dissolution and clay production. To generate a range of rate constants, in each model run we multiplied the rate constants k_X and s_X listed in Table C.1 in the Supplementary data by a single coefficient, which ranged from 0.01–1 between model runs. This approach ensured that the rate constants k_X and s_X remained within the limits of published values for mineral dissolution and clay production, and maintained the same relative magnitudes between model runs. The results in Fig. 6 imply that the stability of $\hat{W}_{inf}$ is not strongly affected by the choice of rate constants for mineral dissolution and clay production, and suggests that chemical denudation rates calculated with Eq. (6) are likely to be accurate over a wide range of mineral dissolution rates and clay production rates.

What does it mean to change the non-dimensional rate constants? The concentration of soluble minerals in the soil is primarily a function of two competing rates: the rate of mineral dissolution (a function of kA) and the rate of fresh mineral supply (a function of α and ϵ_0). Soluble minerals are depleted in the soil more quickly at faster dissolution rates (i.e., at higher values of k) and are replenished more quickly at faster soil production rates (i.e., at higher values of ϵ_0). Soil mineral concentrations thus reflect the balance between mineral dissolution and mineral supply. This suggests that the most important factor controlling soil mineral concentrations is not the absolute values of the mineral dissolution rates, but rather the values of the dissolution rates relative to the soil production rate. A useful means of comparing these rates is by examining the timescales associated with each rate. We define a mineral

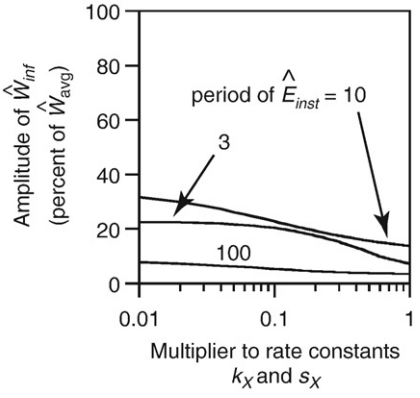

Fig. 6. This depicts the amplitude of $\hat{W}_{inf}$ – defined as the maximum deviation of $\hat{W}_{inf}$ from $\hat{W}_{avg}$ – as a function of the magnitude of the rate constants for mineral dissolution k_X and clay production s_X, relative to their magnitudes in Table C.1 in the Supplementary data. To generate a range of rate constants, in each model run we multiplied the rate constants k_X and s_X in Table C.1 by a single coefficient that ranged from 0.01–1 between model runs. This approach ensured that k_X and s_X maintained the same relative magnitudes between model runs and remained within the range of published values for mineral dissolution and clay production rate constants. During these model runs, we held the amplitude of $\hat{E}_{inst}$ constant at 50% of its mean. This figure suggests that the magnitude of the rate constants for mineral dissolution and clay production have only a small effect on the degree to which inferred chemical denudation rates deviate from average chemical denudation rates during non-steady physical erosion.

dissolution timescale $T_k = k^{-1}A^{-1}$ such that the non-dimensional dissolution rate constant $\widehat{kA}$ is the ratio between the soil production timescale $T_p = \Lambda\epsilon_0^{-1}$ and the mineral dissolution timescale.

$$\widehat{kA} = \frac{kA\Lambda}{\epsilon_0} = \frac{T_p}{T_k} \tag{18}$$

When the soil production timescale T_p is much shorter than the dissolution timescale T_k, fresh soil is produced faster than soluble minerals are depleted in the soil; in this situation, soil mineral concentrations vary little over time and remain close to the mineral concentrations of the parent rock. By contrast, when T_p is much longer than T_k, soluble minerals are depleted from the soil more quickly than soil production can replenish them; in this situation, soil mineral concentrations vary more widely and depend strongly on the rate of soil production.

5.4. Chemical denudation rates at steady physical erosion rates

Up to this point, we have only examined the transient response of inferred chemical denudation rates to non-steady physical erosion rates. Now we consider chemical denudation rates under steady physical erosion rates. This steady-state behavior sheds light on the transient model results, because the response of chemical denudation rates to a shift in physical erosion rates can be understood as a transition from one steady-state chemical denudation rate to another.

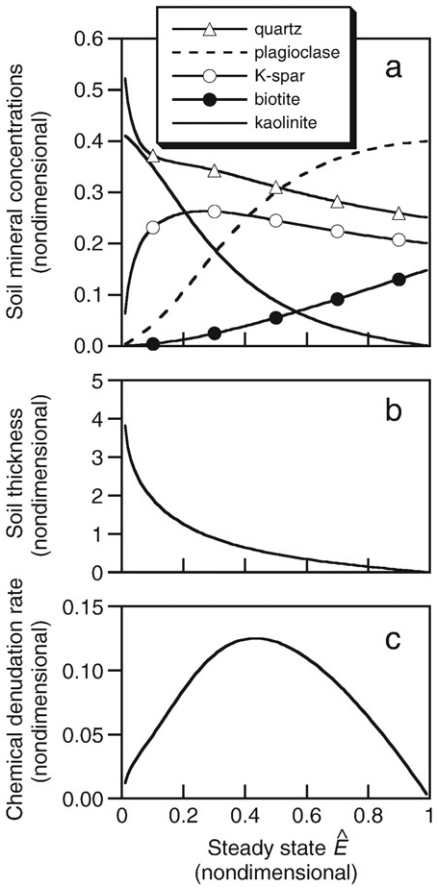

Fig. 7. Soil mineral concentrations, soil thickness, and chemical denudation rates as a function of steady-state physical erosion rate E. Non-dimensional parameter values used in these runs are listed in Table C.2 in the Supplementary data. Chemical denudation rates approach zero at both $\hat{E}\to 0$ and $\hat{E}\to 1$ (i.e., as $E\to 0$ and $E\to\epsilon_0$) because soluble minerals become depleted in the soil as $E\to 0$ and because soil thickness approaches zero as $E\to\epsilon_0$.

According to the model, at any steady physical erosion rate there is a corresponding steady chemical denudation rate. We can calculate steady-state chemical denudation rates by setting the time derivatives in Eqs. (11)–(14) to zero, solving for steady-state soil thickness, CRN and mineral concentrations, and substituting these values into Eq. (15). The results indicate a non-linear dependence of chemical denudation rates on physical erosion rates.

As Fig. 7(c) shows, modeled chemical denudation rates approach zero at both $\hat{E}=0$ and $\hat{E}=1$ (i.e., at $E=0$ and $E=\epsilon_0$), and reach a maximum at an intermediate physical erosion rate. Why does the model predict this relationship?

The non-linear dependence of chemical denudation rates on physical erosion rates can be understood from the variations in soil thickness and soil mineral concentrations in Fig. 7(a) and (b). As physical erosion rates approach the maximum soil production rate (i.e., as $E\to\epsilon_0$), soil thickness shrinks towards zero and soil mineral concentrations approach the concentrations of the parent rock. Conversely, as $E\to 0$, soil thickness increases and the soil residence time increases as well, with the consequence that the more soluble minerals (here plagioclase and biotite) are depleted to a greater extent because they have more time to dissolve. Thus, as physical erosion rates decrease, concentrations of the more soluble minerals decrease too. Our numerical model assumes that the chemical denudation rate of a single mineral phase scales linearly with the mass of that phase in the soil, and that the total chemical denudation rate is the sum of the chemical denudation rates of all the mineral phases. This can be simplified by recognizing that some mineral phases are several orders of magnitude more soluble than others (see the relative solubilities listed in Table C.1 in the Supplementary data), so to first order total chemical denudation rates depend only on the mass of the most soluble mineral phases in the soil. Thus to first order, chemical denudation rates are proportional to the product of the soil mass and the concentration of those soluble minerals in the soil. As concentrations of soluble minerals in the soil approach zero (which occurs as $E\to 0$), chemical denudation rates also approach zero. Similarly, as soil thickness approaches zero (which occurs as $E\to\epsilon_0$), chemical denudation rates also approach zero. In short, the model predicts that chemical denudation rates approach zero at both $E\to 0$ and at $E\to\epsilon_0$ because soluble minerals disappear as $E\to 0$ and the soil itself disappears as $E\to\epsilon_0$.

6. Discussion

The model presented in this paper simulates how soil bulk mineralogy and cosmogenic radionuclide concentrations evolve under forcing by an arbitrary temporal pattern in physical erosion rates. It then compares the "actual" (simulated) chemical denudation rates with those that would be inferred from the concentrations of cosmogenic nuclides and immobile elements. We have primarily used this model to estimate how much inferred rates deviate from actual rates when physical erosion rates vary over time. The model results show that even when physical erosion rates are not steady in time, chemical denudation rates inferred with Eq. (6) should closely approximate actual chemical denudation rates averaged over the timescale of cosmogenic radionuclide accumulation, especially during short-period oscillations in physical erosion rates. When physical erosion rates vary over short timescales (i.e., those on the order of the CRN accumulation time or shorter), the inferred chemical denudation rate W_{inf} is an averager — it smooths out fluctuations in instantaneous chemical denudation rates, and closely resembles the long-term mean. Over long timescales (i.e., those on the order of ten CRN accumulation times or longer), W_{inf} is a follower — it mirrors fluctuations in physical erosion rates. We find that W_{inf} is an accurate recorder of actual chemical denudation rates over a wide range of amplitudes and periods in physical erosion rates and a wide range of mineral dissolution rates and secondary mineral production rates. For

example, given the rate constants for mineral dissolution and soil production used in Table C.1 in the Supplementary data (which, notably, produce soils similar to those in mountainous granitic terrain), the model predicts that when physical erosion rates fluctuate by 50% of the mean, inferred chemical denudation rates deviate from the mean chemical denudation rate averaged over the CRN accumulation timescale by no more than 1% during 1000-year oscillations in physical erosion rates, by 9% during 10,000-year oscillations, and 12% during 100,000-year oscillations. These are the maximum deviations predicted by the model; at most times during the model runs, the discrepancies between inferred and actual chemical denudation rates are smaller.

Is the numerical model outlined in this paper an accurate description of nature? As with any model, it is only as accurate as the assumptions behind it. The major assumptions in the model concern the parameterization of processes that form and erode soil. The first assumption is that soil forms strictly from the bedrock underneath it, and that this process is completely characterized by the soil production function of Heimsath et al. (1997), in which denudation rates decrease exponentially with increasing soil thickness. The second important assumption is that mineral dissolution rates depend only on soil mineral mass, specific surface area, and reactivity. Such a formulation ignores any other factors that might speed or slow dissolution, such as microbial activity, pH, temperature, mineral coatings, and the saturation state of the soil pore water relative to the surrounding minerals. These factors may influence mineral dissolution processes, but they have been left out of the model in the interest of simplicity and tractability. Furthermore, these missing factors may be subsumed in the rate constants for mineral dissolution themselves. Regardless of the influences of these factors, we submit that chemical denudation rates should still scale with the quantity of minerals available to be weathered. Thus, while the model is a highly simplified version of nature, it nonetheless should accurately mimic nature to the degree that the soil production function applies and mineral dissolution rates scale with the total mineral mass in the soil.

Our model also makes a prediction about the steady-state relationship between rates of chemical denudation and physical erosion, a topic of interest in the study of Earth's long-term geomorphic and climatic evolution. Some have theorized that periods of rapid tectonic uplift (and hence rapid physical erosion) might also be marked by rapid chemical weathering because fresh minerals are brought more rapidly to the Earth's surface where weathering occurs (e.g., Raymo et al., 1988). This assumes that chemical weathering rates increase with increasing physical erosion rates. The model outlined in this paper predicts a different relationship; it predicts that chemical denudation rates increase with physical erosion rates, but only up to a point, beyond which chemical denudation rates decrease with further increases in physical erosion rates, a prediction consistent with the hypothesis of Anderson et al. (2002) and the predictions of a landslide model by Gabet (2007). If we drive the model with steady erosion, weathering rates can decline to zero at sufficiently high erosion rates. If instead we drive the model with episodic erosion to mimic the periodic growth and removal of soil under intermittent landsliding, chemical denudation rates can still be greater than zero at very high physical erosion rates because the average soil residence time can be greater than zero. This model prediction also hinges on the assumption that all chemical denudation on hillslopes occurs within the soil; hence as soil thickness approaches zero (in response to very high physical erosion rates), so too chemical denudation rates approach zero. This assumption is not strictly valid because some chemical denudation occurs within the bedrock as groundwater percolates through fractures and dissolves minerals that are highly susceptible to chemical weathering, such as calcite (e.g., White et al., 1999b). However, as long as chemical denudation rates in bedrock are much smaller than chemical denudation rates in soil – as is likely to be the case in granites, which typically contain about 0.1% calcite by mass (White et al., 1999b) – total chemical denudation rates should decrease as physical erosion rates approach soil production rates, as may occur in steep catchments with thin soils. This is a testable prediction, and the degree to which it matches field measurements could indicate how well this model reflects soil formation, denudation, and mineral dissolution under field conditions.

Acknowledgments

We thank two anonymous reviewers and editor R. Carlson for the insightful and constructive comments that significantly improved this manuscript. Our work was supported by a SEGRF fellowship from Lawrence Livermore National Laboratory to K.L.F. and NSF grant EAR-0643129 to J.W.K.

Appendix A. Supplementary data

Supplementary data associated with this article can be found, in the online version, at doi:10.1016/j.epsl.2008.05.024.

References

Anderson, S.P., Dietrich, W.E., Brimhall, G.H., 2002. Weathering profiles, mass-balance analysis, and rates of solute loss: linkages between weathering and erosion in a small, steep catchment Geol. Soc. Amer. Bull. 114 (9), 1143–1158.

Balco, G., Stone, J.O., Lifton, N.A., Dunai, T.J., 2008. A complete and easily accessible means of calculating surface exposure ages or erosion rates from ^{10}Be and ^{26}Al measurements. Quat. Geochr. 3, 174–195.

Berner, R.A., Lasaga, A.C., Garrels, R.M., 1983. The carbonate–silicate geochemical cycle and its effect on atmospheric carbon dioxide over the past 100 million years. Am. J. Sci. 283 (7), 641–683.

Brimhall, G.H., Dietrich, W.E., 1987. Constitutive mass balance relations between chemical composition, volume, density, porosity, and strain in metasomatic hydrochemical systems: results on weathering and pedogenesis Geochim. Cosmochim. Acta 51 (3), 567–587.

Brimhall, G.H., et al., 1992. Deformational mass transport and invasive processes in soil evolution. Science 255 (5045), 695–702.

Busenberg, E., Clemency, C.V., 1976. Dissolution kinetics of feldspars at 25 degrees C and 1 atm CO_2 partial pressure. Geochim. Cosmochim. Acta 40 (1), 41–49.

Chamberlain, C.P., Waldbauer, J.R., Jacobson, A.D., 2005. Strontium, hydrothermal systems and steady-state chemical weathering in active mountain belts. Earth Planet. Sci. Lett. 238 (3–4), 351–366.

Chou, L., Wollast, R., 1984. Study of the weathering of albite at room temperature and pressure with a fluidized bed reactor. Geochim. Cosmochim. Acta 48 (11), 2205–2217.

Gabet, E.J., 2007. A theoretical model coupling chemical weathering and physical erosion in landslide-dominated landscapes. Earth Planet. Sci. Lett. 264, 259–265.

Garrels, R.M., Mackenzie, F., 1967. Origin of the Chemical Compositions of some Springs and Lakes. Advances in Chemistry Series, vol. 67. American Chemical Society, Washington, D.C., pp. 222–242.

Heimsath, A.M., Dietrich, W.E., Nishiizumi, K., Finkel, R.C., 1997. The soil production function and landscape equilibrium. Nature 388 (6640), 358–361.

Heimsath, A.M., Dietrich, W.E., Nishiizumi, K., Finkel, R.C., 1999. Cosmogenic nuclides, topography, and the spatial variation of soil depth. Geomorphology 27 (1–2), 151–172.

Heimsath, A.M., Chappell, J., Dietrich, W.E., Nishiizumi, K., Finkel, R.C., 2000. Soil production on a retreating escarpment in southeastern Australia. Geology 28 (9), 787–790.

Heimsath, A.M., Dietrich, W.E., Nishiizumi, K., Finkel, R.C., 2001. Stochastic processes of soil production and transport: erosion rates, topographic variation and cosmogenic nuclides in the Oregon Coast Range. Earth Surf. Processes Landf. 26 (5), 531–552.

Heimsath, A.M., Furbish, D.J., Dietrich, W.E., 2005. The illusion of diffusion: field evidence for depth-dependent sediment transport. Geology 33 (12), 949–952.

Kirchner, J.W., Granger, D.E., Riebe, C.S., 1997. Cosmogenic isotope methods for measuring catchment erosion and weathering rates. Journal of Conference Abstracts, vol. 2, p. 217.

Lal, D., 1991. Cosmic ray labeling of erosion surfaces: in situ nuclide production rates and erosion models. Earth Planet. Sci. Lett. 104 (2–4), 424–439.

Mudd, S.M., Furbish, D.J., 2006. Using chemical tracers in hillslope soils to estimate the importance of chemical denudation under conditions of downslope sediment transport. J. Geophys. Res.-Earth Surf. 111 (F2). doi:10.1029/2005JF000343.

Press, W.H., Teukolsky, S.A., Vetterling, W.T., Flannery, B.P., 1992. Numerical Recipes in C: The Art of Scientific Computing. Cambridge University Press, New York.

Price, J.R., Velbel, M.A., Patino, L.C., 2005. Rates and time scales of clay-mineral formation by weathering in saprolitic regoliths of the southern Appalachians from geochemical mass balance. Geol. Soc. Am. Bull. 117 (5–6), 783–794.

Raymo, M.E., Ruddiman, W.F., Froelich, P.N., 1988. Influence of late Cenozoic mountain building on ocean geochemical cycles. Geology 16 (7), 649–653.

Riebe, C.S., Kirchner, J.W., Granger, D.E., 2001a. Quantifying quartz enrichment and its consequences for cosmogenic measurements of erosion rates from alluvial sediment and regolith. Geomorphology 40 (1–2), 15–19.

Riebe, C.S., Kirchner, J.W., Granger, D.E., Finkel, R.C., 2001b. Strong tectonic and weak climatic control of long-term chemical weathering rates. Geology 29 (6), 511–514.

Riebe, C.S., Kirchner, J.W., Finkel, R.C., 2003. Long-term rates of chemical weathering and physical erosion from cosmogenic nuclides and geochemical mass balance. Geochim. Cosmochim. Acta 67 (22), 4411–4427.

Riebe, C.S., Kirchner, J.W., Finkel, R.C., 2004a. Sharp decrease in long-term chemical weathering rates along an altitudinal transect. Earth Planet. Sci. Lett. 218 (3–4), 421–434.

Riebe, C.S., Kirchner, J.W., Finkel, R.C., 2004b. Erosional and climatic effects on long-term chemical weathering rates in granitic landscapes spanning diverse climate regimes. Earth Planet. Sci. Lett. 224 (3–4), 547–562.

Small, E.E., Anderson, R.S., Hancock, G.S., 1999. Estimates of the rate of regolith production using Be-10 and Al-26 from an alpine hillslope. Geomorphology 27 (1–2), 131–150.

Stone, J.O.H., Evans, J.M., Fifield, L.K., Allan, G.L., Cresswell, R.G., 1998. Cosmogenic chlorine-36 production in calcite by muons. Geochim. Cosmochim. Acta 62 (3), 433–454.

Walker, J.C.G., Hays, P.B., Kasting, J.F., 1981. A negative feedback mechanism for the long-term stabilization of Earth's surface temperature. J. Geophys. Res.- Oceans Atmos. 86 (NC10), 9776–9782.

White, A.F., Brantley, S.L., 2003. The effect of time on the weathering of silicate minerals: why do weathering rates differ in the laboratory and field? Chem. Geol. 202 (3–4), 479–506.

White, A.F., Blum, A.E., Schulz, M.S., Bullen, T.D., Harden, J.W., Peterson, M.L., 1996. Chemical weathering rates of a soil chronosequence on granitic alluvium: I. Quantification of mineralogical and surface area changes and calculation of primary silicate reaction rates. Geochim. Cosmochim. Acta 60 (14), 2533–2550.

White, A.F., Blum, A.E., Bullen, T.D., Vivit, D.V., Schulz, M., Fitzpatrick, J., 1999a. The effect of temperature on experimental and natural chemical weathering rates of granitoid rocks. Geochim. Cosmochim. Acta 63 (19–20), 3277–3291.

White, A.F., Bullen, T.D., Vivit, D.V., Schulz, M.S., Clow, D.W., 1999b. The role of disseminated calcite in the chemical weathering of granitoid rocks. Geochim. Cosmochim. Acta 63 (13–14), 1939–1953.

Supplementary File to "Effects of physical erosion on chemical denudation rates: a numerical modeling study of soil-mantled hillslopes"

Ken L. Ferrier

Department of Earth and Planetary Science, University of California, Berkeley

Center for Accelerator Mass Spectrometry, Lawrence Livermore National Laboratory, Livermore, CA

James W. Kirchner

Department of Earth and Planetary Science, University of California, Berkeley

Swiss Federal Institute for Forest, Snow, and Landscape Research (WSL), Birmensdorf, Switzerland

Department of Environmental Sciences, Swiss Federal Institute of Technology (ETH), Zürich, Switzerland

---

In the main text, we presented a summary of the model equations and the assumptions underlying them. Here we present the full derivation of all dimensional and nondimensional equations.

A Derivation of model equations

We begin creating the model by deriving an equation for the rate of change in soil thickness H. We assume that mass is added to the soil only by conversion of bedrock to soil from below. Because we are applying mass conservation to a unit column of soil, the dimensions of soil mass are [M L^{-2}].

$$\frac{d(\text{soil mass per unit area})}{dt} = \text{mass input rate} - \text{mass loss rate} \tag{A.1}$$

$$\frac{d(\rho_s H)}{dt} = \epsilon_b - D_{inst} \tag{A.2}$$

Here H is the soil thickness [L], ϵ_b is the rate of bedrock lowering due to conversion of bedrock to soil (also termed the soil production rate) [M L^{-2} T^{-1}], ρ_s is the density of soil [M L^{-3}], and D_{inst} is the denudation rate [M L^{-2} T^{-1}], defined as the rate of soil mass loss per unit area. We assume that the soil production rate ϵ_b depends exponentially on soil thickness as in the formulation of *Heimsath et al.* (1997, 1999, 2000, 2001, 2005).

$$\epsilon_b = \epsilon_0 e^{-\alpha H} \tag{A.3}$$

Here ϵ_0 represents the soil production rate in the absence of soil, and α [L^{-1}] is a constant that describes the exponential dependence of soil production rate on soil thickness. If we assume ρ_s is constant in time and that D_{inst} is the sum of instantaneous physical erosion rates E_{inst} and instantaneous chemical denudation rates W_{inst}, then the rate of change in soil thickness H is:

$$\frac{dH}{dt} = \frac{1}{\rho_s}(\epsilon_0 e^{-\alpha H} - E_{inst} - W_{inst}). \tag{A.4}$$

Noting that in a well-mixed soil the CRN concentration N_s [atoms M^{-1}] is the total number of CRN atoms in the soil column, n_s [atoms L^{-2}], divided by the mass of the soil column, $\rho_s H$ [M L^{-2}], and assuming that ρ_s is constant in time,

$$\frac{dN_s}{dt} = N_s(\frac{1}{n_s}\frac{dn_s}{dt} - \frac{1}{H}\frac{dH}{dt}). \tag{A.5}$$

We then assume that the soil gains CRN only through in-situ production of CRN and through incorporation of CRN from bedrock during soil production at the soil-bedrock boundary, and loses CRN only through soil denudation.

$$\begin{aligned}\frac{dn_s}{dt} = &\frac{dn_s}{dt}(\text{in-situ CRN production}) + \frac{dn_s}{dt}(\text{soil production}) \\ &-\frac{dn_s}{dt}(\text{loss to denudation})\end{aligned} \tag{A.6}$$

Because Equation A.6 neglects radioactive decay, it is suitable for stable CRN (^{3}He, ^{21}Ne) and CRN with half-lives that are much longer than the residence time of minerals within the penetration depth of cosmogenic radiation (^{10}Be, ^{26}Al), and unsuitable for CRN with much shorter half-lives (e.g., ^{14}C). The production rate of CRN in the soil decreases exponentially with depth, and thus the in-situ production rate of CRN in the soil column is, expressed in [atoms L^{-2} T^{-1}],

$$\frac{dn_s}{dt}(\text{in-situ CRN production}) = \rho_s \int_0^H P_0 e^{-\rho_s z/\Lambda} dz$$
$$= \Lambda P_0 (1 - e^{-\rho_s H/\Lambda}). \quad \text{(A.7)}$$

Defining N_{z_b} as the concentration of CRN in bedrock at the soil-bedrock boundary at depth z_b, the rate of CRN supply to the soil by soil production is N_{z_b} times the soil production rate:

$$\frac{dn_s}{dt}(\text{soil production}) = N_{z_b} \epsilon_0 e^{-\alpha H}. \quad \text{(A.8)}$$

N_{z_b} varies in time as the cosmic ray flux produces new CRN at the soil-bedrock boundary (the first term in Equation A.9) and as soil production pushes the soil-bedrock boundary deeper below the surface where CRN concentrations are smaller (the second term).

$$\frac{dN_{z_b}}{dt} = P(z_b) + \frac{\epsilon_0 e^{-\alpha H}}{\rho_r} \Big(\frac{\partial N(z \geq z_b)}{\partial z} \Big) \quad \text{(A.9)}$$

Because the CRN production rate drops off exponentially as it passes through matter, and because CRN concentrations below the soil-bedrock boundary drop off exponentially according to Equation A.10,

$$N(z \geq z_b) = N_{z_b} e^{-\rho_r (z - z_b)/\Lambda}, \quad \text{(A.10)}$$

the rate of change of N_{z_b} over time is given by:

$$\frac{dN_{z_b}}{dt} = P_0 e^{-\rho_s H/\Lambda} - \epsilon_0 e^{-\alpha H} \frac{N_{z_b}}{\Lambda}. \quad \text{(A.11)}$$

The loss of CRN through soil denudation is the soil CRN concentration N_s times the denudation rate.

$$\frac{dn_s}{dt}(\text{loss to denudation}) = N_s D_{inst}$$
$$= N_s (\epsilon_0 e^{-\alpha H} - \rho_s \frac{dH}{dt}) \quad \text{(A.12)}$$

The rate of change of n_s is thus

$$\frac{dn_s}{dt} = \Lambda P_0 (1 - e^{-\rho_s H/\Lambda}) + N_{z_b} \epsilon_0 e^{-\alpha H} - N_s (\epsilon_0 e^{-\alpha H} - \rho_s \frac{dH}{dt}), \quad \text{(A.13)}$$

which can be substituted into Equation A.5 to yield an expression for CRN concentrations in a well-mixed soil.

$$\frac{dN_s}{dt} = \frac{1}{\rho_s H}\Big(\epsilon_0 e^{-\alpha H}(N_{z_b} - N_s) + \Lambda P_0(1 - e^{-\rho_s H/\Lambda})\Big) \tag{A.14}$$

Lastly, we derive an expression for the rate of change of mineral concentrations in the soil column. We define the average concentration of mineral X in soil, $[X]_s$ [mol M^{-1}], as the number of moles of mineral X in the soil column, Q_X [mol L^{-2}], divided by the mass of the soil column, $\rho_s H$ [M L^{-2}]. Thus the rate of change of $[X]_s$ is, assuming a constant soil density,

$$\frac{d[X]_s}{dt} = \frac{1}{\rho_s H}(\frac{dQ_X}{dt} - [X]_s \rho_s \frac{dH}{dt}). \tag{A.15}$$

We now derive an expression for dQ_X/dt to substitute into Equation A.15 by applying conservation of mass to mineral X in the soil column:

$$\begin{aligned}\frac{dQ_X}{dt} = &\frac{dQ_X}{dt}(\text{soil production}) + \frac{dQ_X}{dt}(\text{mineral generation}) \\ &-\frac{dQ_X}{dt}(\text{mineral dissolution}) - \frac{dQ_X}{dt}(\text{physical erosion}).\end{aligned} \tag{A.16}$$

In this expression the first two terms represent inputs of mineral X to the soil, and the last two terms represent losses of mineral X from the soil. The first term is the rate at which mineral X is supplied to the soil by conversion of bedrock to soil, and is given by Equation A.17, in which $[X]_r$ is the concentration of X in bedrock.

$$\frac{dQ_X}{dt}(\text{soil production}) = \epsilon_0 e^{-\alpha H}[X]_r \tag{A.17}$$

This second term is the rate of mineral production within the soil, and we assume it to be nonzero only for secondary minerals. We follow *Chamberlain et al.* (2005) in defining s_X to be the rate of secondary mineral production per unit volume [mol L^{-3} T^{-1}], such that the total rate of secondary mineral production in the soil column is

$$\frac{dQ_X}{dt}(\text{mineral generation}) = s_X H. \tag{A.18}$$

The third term is the rate of mineral dissolution, and we follow the approach of *Chamberlain et al.* (2005) in modeling the dissolution rate of mineral phase

X as a linear function of its specific surface area A_X [L^2 mol^{-1}] and its concentration in the soil $[X]_s$ [mol M^{-1}].

$$\frac{d[X]_s}{dt}(\text{mineral dissolution}) = -k_X A_X [X]_s \tag{A.19}$$

Here k_X is the dissolution rate constant [mol L^{-2} T^{-1}]. Over the entire soil column, the total number of moles of mineral X lost to dissolution is then

$$\frac{dQ_X}{dt}(\text{mineral dissolution}) = -k_X A_X [X]_s \rho_s H. \tag{A.20}$$

For all primary minerals we calculate specific surface area A_X as

$$A_X = \frac{6 R_X w_X}{\rho_X d_X} \tag{A.21}$$

following *White* (1995), where ρ_X is the density of mineral X [M L^{-3}], w_X is the molar mass of mineral X [M mol^{-1}], d_X is the grain diameter of mineral X [L], and R_X is the surface roughness of mineral X [unitless], which we calculate following *Anbeek et al.* (1994). For secondary minerals, which tend to be much smaller and hence have much larger specific surface areas, we use empirically-determined specific surface areas. Table C.1 provides a list of published values for each of these parameters.

Lastly, the fourth term of the mass balance in Equation A.16 is the number of moles of mineral X lost by physical erosion of soil, and is given by the physical erosion rate times the concentration of mineral X in the soil.

$$\frac{dQ_X}{dt}(\text{physical erosion}) = -E_{inst} [X]_s \tag{A.22}$$

Substitution of Equations A.17, A.18, A.20, and A.22 into Equation A.16 yields the following expression for dQ_X/dt.

$$\frac{dQ_X}{dt} = \epsilon_0 e^{-\alpha H} [X]_r + s_X H - k_X A_X [X]_s \rho_s H - E_{inst} [X]_s \tag{A.23}$$

Finally, substitution of Equations A.23, A.4, and 15 into Equation A.15 yields the rate of change in the concentration of mineral X (Equation A.24). We use Equation A.24 to calculate the evolution of all soil mineral concentrations over time, including the concentration of an insoluble mineral, a quantity that is needed to infer chemical denudation rates via Equation 6.

$$\frac{d[X]_s}{dt} = \frac{\epsilon_0 e^{-\alpha H}}{\rho_s H}([X]_r - [X]_s) + \frac{s_X}{\rho_s} - k_X A_X [X]_s + [X]_s \sum_{j=1}^{n} (k_j A_j [X_j]_s w_j - \frac{s_j w_j}{\rho_s}) \quad \text{(A.24)}$$

Here n is the number of mineral phases in the soil, $[X_j]_s$ is the concentration of the j^{th} soil mineral phase in the summation [mol M^{-1}], and k_j, A_j, s_j, and w_j are the dissolution rate constant, specific surface area, secondary mineral production rate, and molar mass, respectively, of the j^{th} mineral phase in the summation.

B Derivation of nondimensional model equations

The dimensional differential equations for H, N_s, N_{z_b}, and $[X]_s$ depend on a number of independent parameters. Here we nondimensionalize these equations to remove the model's dependence on soil production parameters ϵ_0 and α and on CRN production parameters P_0 and Λ in order to clarify the dominant controls on soil thickness, CRN concentrations, and soil mineral concentrations. We do not ascribe particular meaning or importance to the nondimensionalizations presented here; we applied these nondimensionalizations merely to eliminate particular dimensional parameters. We note that other nondimensionalization schemes are possible, and that in all schemes nondimensional parameters are easily scaled back to their dimensional counterparts.

We begin nondimensionalizing the model by noting that time can be scaled by a soil production timescale $T_P = \Lambda \epsilon_0^{-1}$, such that nondimensional time $\hat{t}$ is given by

$$\hat{t} = \frac{t}{T_P} = \frac{t\epsilon_0}{\Lambda}. \quad \text{(B.1)}$$

Here and below we denote nondimensional quantities with a carat. We nondimensionalize soil density by dividing by $\alpha\Lambda$,

$$\hat{\rho}_s = \frac{\rho_s}{\alpha\Lambda}, \quad \text{(B.2)}$$

and scale soil depth with the soil production parameter α.

$$\hat{H} = H\alpha \quad \text{(B.3)}$$

We nondimensionalize CRN concentrations N_{z_b} and N_s by scaling them to the hypothetical soil CRN concentration that would occur at a steady-state denudation rate of the maximum soil production rate ϵ_0.

$$\hat{N}_{z_b} = \frac{N_{z_b}\epsilon_0}{P_0\Lambda}, \hat{N}_s = \frac{N_s\epsilon_0}{P_0\Lambda} \tag{B.4}$$

Molar mineral concentrations are scaled by their molar masses to yield nondimensional concentrations

$$[\hat{X}]_r = [X]_r w_X, [\hat{X}]_s = [X]_s w_X, \tag{B.5}$$

and mineral dissolution and production parameters are scaled as follows.

$$\hat{k}_X = \frac{k_X w_X}{\epsilon_0}, \hat{A}_X = \frac{A_X\Lambda}{w_X}, \hat{s}_X = \frac{s_X w_X \Lambda}{\rho_s \epsilon_0} \tag{B.6}$$

Here $\hat{k}_X$ is the ratio of the dissolution rate of mineral phase X to the maximum soil production rate ϵ_0, $\hat{A}_X$ is the specific surface area of X relative to the inverse of the gamma-ray neutron penetration depth, and $\hat{s}_X$ relates the clay production rate of X to the maximum soil production rate ϵ_0. We lastly scale all inferred and instantaneous denudation and erosion rates by the maximum soil production rate ϵ_0.

$$\begin{aligned}
\hat{E}_{inst} &= \frac{E_{inst}}{\epsilon_0} \\
\hat{D}_{inf} &= \frac{D_{inf}}{\epsilon_0} = \frac{1}{\hat{N}_s} \\
\hat{W}_{inf} &= \frac{W_{inf}}{\epsilon_0} = \frac{1}{\hat{N}_s}\Big(1 - \frac{[\hat{Z}r]_r}{[\hat{Z}r]_s}\Big) \\
\hat{W}_{inst} &= \frac{W_{inst}}{\epsilon_0} = \hat{\rho}_s \hat{H} \sum_{j=1}^{n} (\hat{k}_j \hat{A}_j [\hat{X}_j]_s - \hat{s}_j)
\end{aligned} \tag{B.7}$$

Under the transformations in Equations B.1-B.7, the governing equations assume the following nondimensional forms.

$$\frac{d\hat{H}}{d\hat{t}} = \frac{1}{\hat{\rho}_s}\Big(e^{-\hat{H}} - \hat{E}_{inst} - \hat{\rho}_s \hat{H} \sum_{j=1}^{n} (\hat{k}_j \hat{A}_j [\hat{X}_j]_s - \hat{s}_j)\Big) \tag{B.8}$$

$$\frac{d\hat{N}_{z_b}}{d\hat{t}} = e^{-\hat{\rho}_s \hat{H}} - \hat{N}_{z_b} e^{-\hat{H}} \tag{B.9}$$

$$\frac{d\hat{N}_s}{d\hat{t}} = \frac{1}{\hat{\rho}_s \hat{H}}\Big(e^{-\hat{H}}(\hat{N}_{z_b} - \hat{N}_s) + 1 - e^{-\hat{\rho}_s \hat{H}}\Big) \tag{B.10}$$

$$\frac{d[\hat{X}]_s}{d\hat{t}} = \frac{e^{-\hat{H}}}{\hat{\rho}_s \hat{H}}([\hat{X}]_r - [\hat{X}]_s) + \hat{s}_X - \hat{k}_X \hat{A}_X [\hat{X}]_s + [\hat{X}]_s \sum_{j=1}^{n} (\hat{k}_j \hat{A}_j [\hat{X}_j]_s - \hat{s}_j) \tag{B.11}$$

C Tables of parameter values used in model runs

Table C.1
Mineral parameter values used in Figure 2

Mineral[a]	Molar mass w ($\frac{g}{mol}$)	Density ρ ($\frac{kg}{m^3}$)	Dissolution rate[b] k ($\frac{mol}{m^2\ yr}$)	Production rate[c] s ($\frac{mol}{m^3\ yr}$)	Surface roughness[d] R	Surface area[e] A ($\frac{m^2}{mol}$)	Relative Solubility[f] $kA/(kA)_{qz}$
Quartz	60.09	2650	5.0×10^{-8}	0	3	2	1
Plagioclase	265.44	2650	5.0×10^{-6}	0	39	117	5465
K-feldspar	278.35	2560	5.0×10^{-7}	0	8	26	122
Biotite	464.60	3090	2.0×10^{-6}	0	237	1069	19690
Zircon	183.31	4600	0	0	3	4	0
Kaolinite	258.18	2600	5.0×10^{-8}	0.51	n/a	4776	2234

[a] We model plagioclase as a standard oligoclase (20% Ca, 80%Na), and assume biotite has the stoichiometric formula $KMg_{1.5}Fe_{1.5}Si_3AlO_{10}(OH)_2$.

[b] We use field-based dissolution rate constants for plagioclase, K-feldspar and biotite from *Clow and Drever* (1996), the mean field-based dissolution rate constant from *Schulz and White* (1999) for quartz, and assume zircon is insoluble. In the absence of field-based dissolution rate constants for kaolinite, we assume that the ratio of $k_{kaolinite}$ to $k_{oligoclase}$ in the field is the same as the ratio measured in lab experiments (*Cama et al.*, 2002; *Huertas et al.*, 1999; *White and Brantley*, 2003); that is, we assume that $k_{kaolinite}$ is two orders of magnitude lower than the field-based $k_{oligoclase}$.

[c] We assume that the mineral production rate in the soil is zero for each primary mineral, and we use a kaolinite production rate of 0.1 g kg^{-1} yr^{-1}, a value that falls within the range of 0.001-0.2 g kg^{-1} yr^{-1} given in *Barshad* (1957), as cited by *Price et al.* (2005).

[d] We calculate surface roughness for each primary mineral following *Anbeek et al.* (1994).

[e] For each primary mineral we calculate surface area as $A = 6Rw\rho^{-1}d^{-1}$ following *White* (1995), where d is the mineral grain diameter, which we assume to be 200 microns. Because secondary kaolinite crystals are generally much smaller than 200 microns, we use an experimentally-determined surface area for kaolinite (*Cama et al.*, 2002).

[f] The relative solubility here is the product of the dissolution rate constant k and the specific surface area A, scaled by the product of k and A for quartz.

Table C.2
Nondimensional parameter values used in Figures 3-7

	$[\hat{X}]_r$	$\hat{k}$	$\hat{A}$	$\hat{s}$
quartz	0.2499	8.0×10^{-9}	3.1×10^{4}	0
plagioclase	0.4000	3.6×10^{-6}	3.9×10^{5}	0
K-feldspar	0.2000	3.7×10^{-7}	8.3×10^{4}	0
biotite	0.1500	2.5×10^{-6}	2.0×10^{6}	0
zircon	0.0001	0	1.8×10^{4}	0
kaolinite	0	3.5×10^{-8}	1.6×10^{7}	0.43
$\hat{\rho}_s = 0.276$				

References

Anbeek, C., N. van Breemen, E. L. Meijer, and L. van der Plas (1994), The dissolution of naturally weathered feldspar and quartz, *Geochimica et Cosmochimica Acta*, *58*(21), 4601–4613.

Barshad, I. (1957), Factors affecting clay formation, in *Proceedings of the 6th National Conference on Clays and Clay Minerals*, pp. 110–132, National Academy of Sciences – National Research Council, Washington, D.C.

Cama, J., V. Metz, and J. Ganor (2002), The effect of pH and temperature on kaolinite dissolution rate under acidic conditions, *Geochimica et Cosmochimica Acta*, *66*(22), 3913–3926.

Chamberlain, C. P., J. R. Waldbauer, and A. D. Jacobson (2005), Strontium, hydrothermal systems and steady-state chemical weathering in active mountain belts, *Earth and Planetary Science Letters*, *238*(3-4), 351–366.

Clow, D. W., and J. I. Drever (1996), Weathering rates as a function of flow through an alpine soil, *Chemical Geology*, *132*(1-4), 131–141.

Heimsath, A. M., W. E. Dietrich, K. Nishiizumi, and R. C. Finkel (1997), The soil production function and landscape equilibrium, *Nature*, *388*(6640), 358–361.

Heimsath, A. M., W. E. Dietrich, K. Nishiizumi, and R. C. Finkel (1999), Cosmogenic nuclides, topography, and the spatial variation of soil depth, *Geomorphology*, *27*(1-2), 151–172.

Heimsath, A. M., J. Chappell, W. E. Dietrich, K. Nishiizumi, and R. C. Finkel (2000), Soil production on a retreating escarpment in southeastern Australia, *Geology*, *28*(9), 787–790.

Heimsath, A. M., W. E. Dietrich, K. Nishiizumi, and R. C. Finkel (2001), Stochastic processes of soil production and transport: Erosion rates, topographic variation and cosmogenic nuclides in the Oregon Coast Range, *Earth Surface Processes and Landforms*, *26*(5), 531–552.

Heimsath, A. M., D. J. Furbish, and W. E. Dietrich (2005), The illusion of

diffusion: Field evidence for depth-dependent sediment transport, *Geology*, *33*(12), 949–952.

Huertas, F. J., L. Chou, and R. Wollast (1999), Mechanism of kaolinite dissolution at room temperature and pressure Part II: Kinetic study, *Geochimica et Cosmochimica Acta*, *63*(19-20), 3261–3275.

Price, J. R., M. A. Velbel, and L. C. Patino (2005), Rates and time scales of clay-mineral formation by weathering in saprolitic regoliths of the southern Appalachians from geochemical mass balance, *Geological Society of America Bulletin*, *117*(5-6), 783–794.

Schulz, M. S., and A. F. White (1999), Chemical weathering in a tropical watershed, Luquillo Mountains, Puerto Rico III: Quartz dissolution rates, *Geochimica et Cosmochimica Acta*, *63*(3-4), 337–350.

White, A. F. (1995), Chemical weathering rates in soils, *Reviews in Mineralogy*, *31*, 407–461.

White, A. F., and S. L. Brantley (2003), The effect of time on the weathering of silicate minerals: why do weathering rates differ in the laboratory and field?, *Chemical Geology*, *202*(3-4), 479–506.